processes

MDPI

Article

Electron Microscopy Reveals Variation in Starch Granules in Rice Grains Related to Glycemic Index

Shubha Banerjee [1,*,†], Amiruddin Ali [1,*,†], Maqbool Qutub [1], Shivani Singh Rana [1], Pradnya Raut [1], Vipin Kumar Pandey [1], Mustafa N [1], Taruna Borule [1], Nagaraju Dharavath [2] and Karthikeyan Adhimoolam [3]

[1] Department of Plant Molecular Biology and Biotechnology, Indira Gandhi Krishi Vishwavidyalaya, Raipur 492012, Chhattisgarh, India
[2] Department of Genetics and Plant Breeding, Indira Gandhi Krishi Vishwavidyalaya, Raipur 492012, Chhattisgarh, India
[3] Subtropical Horticulture Research Institute, Jeju National University, Jeju 63243, Republic of Korea
* Correspondence: shubha.banerjee@igkv.ac.in (S.B.); amiruddinali786786@gmail.com (A.A.)
† These authors contributed equally to this work.

Abstract

The glycemic index (GI) of rice is a complex trait, affected by amylose content (AC), size, and packaging of starch granules (SGs). In this study, the electron microscopy results of starch morphology of nine rice genotypes showed varying AC (6.93–36.9%), and the predicted GI (pGI: 41.07–82.46) in relation to genetic factors revealed that smaller SG surface area (20.06 μm^2) and irregular morphology (Hap 3-3 P-11, pGI = 41.07) were associated with a lower pGI, while larger SG surface area (47.68 μm^2) and spherical structure were associated with a higher pGI (NON-HAI, pGI = 82.46). The expression of starch biosynthesis and packaging-related genes (*OsSSIIb*, *OsSSIIc*, *OsSBEIIa*, *OsISA1*, *OsISA3*, *OsGBP*, *OsFLO6*, and *OsBT1*) revealed downregulation of *OsGBP* and *OsISA3* genes in low pGI lines IRRI-147 (pGI = 56.2) and Hap 3-1-p-18 (pGI = 41.79), respectively, while higher levels of expression of the *OsBT1* gene in Makro (pGI = 59.06) and *OsSSIIb* in Swarna (pGI = 58.06) were observed. All these genotypes had similar AC (~30%), but the difference in expression pattern was correlated with starch granule morphology, suggesting its role in influencing pGI. Further, analysis of allelic variation in eight starch-related genes across 20 rice genotypes showed that allelic variants of only *OsGBP* were correlated with AC, where allele group 2 showed lower AC (9.62%), while all other allele groups showed consistently high AC (22–24%). These findings underscore the critical role of starch granule morphology and *OsGBP* allelic variation in determining AC and GI, providing actionable insights for developing low GI rice varieties using tools like CRISPR.

Keywords: glycemic Index; amylose content; starch granules; OsGBP; allelic variation; starch packaging; CRISPR

Academic Editor: Elzbieta Klewicka

Received: 4 May 2025
Revised: 29 June 2025
Accepted: 22 July 2025
Published: 11 October 2025

Citation: Banerjee, S.; Ali, A.; Qutub, M.; Rana, S.S.; Raut, P.; Pandey, V.K.; N, M.; Borule, T.; Dharavath, N.; Adhimoolam, K. Electron Microscopy Reveals Variation in Starch Granules in Rice Grains Related to Glycemic Index. *Processes* **2025**, *13*, 3241. https://doi.org/10.3390/pr13103241

1. Introduction

The glycemic index (GI) is a complex trait targeted in recent rice breeding programs as it depends on the rate of glucose release following the hydrolysis of starch present in grains [1]. Rice, a staple for over half the global population, predominantly consists of starch composed of amylose and amylopectin, whose structural and compositional attributes directly influence digestibility and glycemic index (GI) [2]. While low-GI rice varieties, characterized by elevated amylose content (AC > 22%), offer nutritional benefits,

their adoption is hindered by undesirable organoleptic properties, such as hard texture and bold grains, which conflict with modern rice improvement efforts.

Starch in rice grain is composed of approximately one-quarter amylose and three-quarters amylopectin. Amylopectin is highly branched polymer of glucose with α-1, 6 glycosidic linkages in addition to α-1, 4 linkages (usually found in amylose). Amylopectin is a highly organized molecule in which glucose chains are clusters, giving the molecule distinct architectural and genotypic specificity. The long chains of amylopectin often form crystalline structures that are resistant to hydrolysis, likely due to stabilization in helical forms with hydrogen bonds [3,4]. Starch granules, with higher surface-to-volume ratios, facilitate rapid starch breakdown, correlating with elevated GI [5]. Conversely, granules with lower surface-to-volume ratio and higher amylose content slow digestion, reducing GI but often compromising texture. Furthermore, the synthesis and organization of amylopectin, governed by genes such as *SSIIa*, *SBEIIb*, and *GBSSI*, dictate starch crystallinity and resistance to hydrolysis [6–9]. With the advent of CRISPR technology, starch synthesis pathway genes such as *GBSSI* (*Wx*), *SSIIa*, and *SBEII*, catalyzing synthesis of granule-bound, soluble starch and inducing branching in the amylose, have been targeted to develop low-GI rice varieties [8,10,11].

Although progress has been made in the development of rice varieties with a low glycemic index (GI), numerous challenges continue to exist, especially in relation to their sensory characteristics. These types frequently display unfavorable characteristics, including longer cooking times, increased hardness of the grains, and a more pronounced grain texture. Furthermore, they generally exhibit lower stickiness, increased water absorption rates, and decreased overall taste appeal, which result in a lower preference among consumers. It is essential to tackle these sensory and textural issues to promote greater acceptance of low-GI rice among consumers [12–15]. Furthermore, regional culinary preferences complicated breeding objectives. High GI japonica varieties are mostly preferred in northern China, while medium GI indica rice prevails in southern China and India, reflecting divergent consumer priorities [16,17].

In view of the current understanding of starch synthesis, packaging, and transport in rice grains, the genomic regions responsible for cooking quality of rice, this study investigated nine rice genotypes, including near-isogenic lines (NILs) and commercial varieties, to unravel the genetic and morphological factors influencing the glycemic index (GI). We analyzed the starch granule (SG) surface area, the amylose content (AC), and the expression profiles of key starch biosynthesis genes (*OsSSIIb*, *OsGBP*, *OsFLO6*, *OsISA1*, etc.). Additionally, the correlation between amylose content and various grain properties, including grain width, starch granule size (starch surface area), water uptake ratio, and gel consistency, was determined. The current study was undertaken to understand the effect of size of starch granule (SG) surface area on grain quality parameters and to identify the target genes that can be edited to develop low GI rice varieties without bringing adverse changes in grain morphology and consumer preferences [18,19]. This challenge highlights the importance of distinguishing the genetic and biochemical factors influencing glycemic index (GI) from those affecting sensory quality. Emerging imaging and microfluidic technologies (e.g., advanced optical lenses or on-chip sorting) promise higher-throughput starch analysis in the future. However, such platforms have little application to crop starch phenotyping; current studies still rely on electron and light microscopy to resolve granule size and structure [20,21]. Thus, this study promises to identify suitable candidate genes for a CRISPR-based approach to modifying the glycemic index without losing its consumer value.

2. Materials and Methods

2.1. Plant Materials

Nine rice genotypes were used for the present study, including IRRI-147, NON-HAI: IRGC 29636-2, Amber: IRGC 275-22-1(332/193), Swarna, Makro, Hap 3-3 P-11, Hap 3-1 P-22, Hap 3-1P-18, and M-55. Of these, three are near-isogenic lines (NILs), viz. Hap 3-3 P-11, Hap 3-1 P-22, and Hap 3-1P-18 (cross of Swarna and Aus 329), and six are well-known commercial varieties (Figure 1). The genotypes were selected based on glycemic index value and amylose content. The Haplo-NILs were developed and selected based on low pGI value and presence of desirable alleles, as part of the previous study conducted in the DBT-funded collaborative project (title: "Development of superior haplotype based near isogenic lines (Haplo-NILs) for enhanced genetic gain in rice" 2019–2023). All the seeds were obtained from the ISARC (IRRI South Asia Regional Centre), Varanasi, IRRI, as part of the collaborative research project on superior haplotypes of rice (Figure 1).

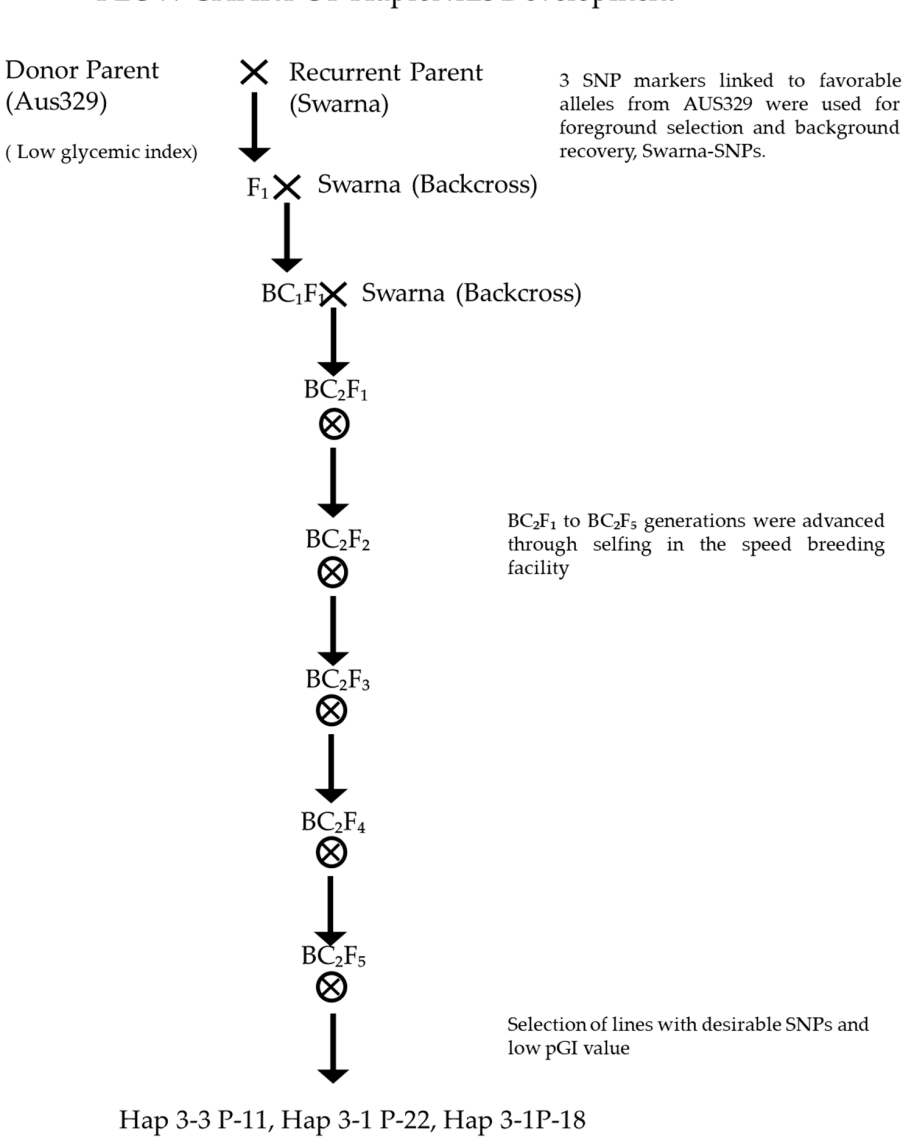

Figure 1. Flow chart of HaploNILs (Hap 3-3 P-11, Hap 3-1 P-22, and Hap 3-1P-18) development. SNP markers (snpOS01104, snpOS01105, snpOS01107, and snpOS01109) linked to favorable alleles from AUS329 at LOC_Os08g12590 were used for foreground selection in the Swarna × AUS329 breeding program under the HaploNILS project. Speed breeding was performed at a speed breeding facility at ISARC, Varanasi, India.

2.2. Preparation and Extraction of Starch

To study the rice starch granule structure, starch was first extracted using the method described by Qin et al. [22]. A total of 10 g of rice flour was initially added to 20 mL of 0.1% NaOH solution, and the mixture was incubated at 4 °C for 18 h. The suspension was subsequently homogenized for 2 min to ensure complete mixing. The suspension was then centrifuged at 10,000 rpm for 10 min to isolate the starch, which was then cautiously collected and washed with distilled water and 0.1% NaOH. In the next step, an equal amount of 1 N HCl (pH = 6.5) was added to each sample to neutralize, and centrifugation was performed at 10,000 rpm for 10 min. The starch was then washed with distilled water, collected, dried, powdered, and sieved, and to maintain its integrity, the sample was kept at 4 °C.

2.3. Scanning Electron Microscopy (SEM)

A scanning electron microscope (SEM; Carl Zeiss, Oberkochen, Germany, UHR FESEM Model GeminiSEM 500 KMAT) operating at 5000X magnification was used to examine the size and distribution of the isolated starch granules. Each sample of two replicates was coated with a thin layer of gold prior to imaging to improve conductivity. The average size and size distribution of the starch granules were then determined from the SEM images using the open-source software ImageJ v1.54k.

2.4. Estimation of Different Starch Biochemical Properties of Rice

2.4.1. Amylose Content

The amylose content in the sample was estimated using the Juliano method [23]. First, a 100 mL volumetric flask was taken, and then 0.1 g of rice flour, 9 mL of 1 N NaOH, and 1 mL of 95% ethanol were added. The mixture was stirred thoroughly and then boiled at 100 °C in a water bath for 15 min. After cooling, the volume was 100 mL after adding 90 mL of distilled water (DW). Next, a 5 mL aliquot was transferred to a new volumetric flask, where 1 mL of 1 N acetic acid and 0.2% of 2 mL iodine solution were added. The volume was increased to 100 mL (8 mL sample and 92 mL DW), and the flask was covered with a dark cloth and incubated in the dark at room temperature for 20 min. Finally, absorbance was recorded at 620 nm using a spectrophotometer.

$$\text{Amylose \% } (x) = \frac{y - 0.2138}{0.0168}$$

where y is the absorbance value.

2.4.2. Total Starch

To analyze the starch content, 100 mg of rice flour was first measured. Subsequently, 0.1 mL of thermostable alpha-amylase (280 U) and 10 mL of sodium acetate buffer were added, followed by vortex mixing. The mixture was vortexed every five minutes during 30 min of incubation at 100 °C in a sealed tube. After incubation, samples were cooled for 5 min in a water bath set at 50 °C. Next, 0.1 mL of Amyloglucosidase (AMG) (330 U) was added, and the samples were incubated at 50 °C for another 30 min. For analysis, a 2 mL aliquot of the test solution was centrifuged at 13,000 rpm for 5 min using a microcentrifuge tube. The resulting 1 mL samples were then diluted 11-fold by adding 10 mL of sodium acetate buffer. Later, the GOPOD test was performed by adding 3.0 mL of GOPOD reagent to 0.1 mL aliquots of the solutions. Absorbance was measured at 510 nm against a reagent blank after 20 min of incubation at 50 °C. Control analyses were conducted for each sample under the same incubation conditions, using 0.2 mL of 100 mM sodium acetate buffer with $CaCl_2$ in place of the thermostable alpha-amylase and AMG [24].

2.4.3. Glycemic Index

The glycemic index (GI) of rice flour was determined using a modified protocol from Goni et al. [25]. First, 50 mg of rice flour was mixed with 5 mL of water and boiled in a water bath for 30 min. The mixture was then incubated at 40 °C for 1 h with 10 mL of HCl-KCl buffer (pH 1.5) and 0.2 mL of pepsin. The volume was adjusted to 25 mL with Tris-malate buffer (pH 6.9) and further incubated at 37 °C in a water bath with 5 mL of α-amylase (2.6 units) in Tris-malate buffer (pH 6.9). Aliquots of 1 mL were collected at 30, 60, 90, and 120 min, and enzyme activity was inactivated by heating at 100 °C for 5 min. After cooling, 3 mL of 0.4 M sodium acetate buffer was added to the sample aliquots, which were then incubated for 30, 60, 90, and 120 min. To hydrolyze the digested starch to glucose, 60 µL of amyloglucosidase (AMG) was added, and the mixture was incubated at 60 °C for 45 min in a water bath. Subsequently, 3 mL of GOPOD Reagent was added to the amber-colored tubes containing 100 µL of the sample aliquot and incubated at 40 °C for 20 min. Absorbance was measured at 510 nm using a spectrophotometer, with a blank and a glucose standard used for calibration. For calculating pGI, a non-linear first-order equation developed by Goni et al. was used: $C = C\alpha\ (1 - e^{-kt})$, where C is the concentration of starch hydrolyzed at the time (t), $C\alpha$ is the equilibrium concentration (i.e., % of starch hydrolyzed after 180 min, which is the glucose content after 120 min divided by the total starch), and k is the kinetic constant. The area under the hydrolysis curve (AUC) was calculated using the equation $AUC = C\alpha_{(tf-t0)} - C\alpha/k\ (1 - e^{-k(tf-t0)})$, where $C\infty$ is the concentration at equilibrium (t_{120}), t_f is the final time (120 min), t_0 is the initial time (0 min), and k is the kinetic constant. A hydrolysis index (HI) was calculated by comparison with the AUC of a reference food (white bread and cane sugar). The predicted glycemic index (PGI) was estimated using the formula pGI = 39.7 + 0.548 (HI) [16].

2.4.4. Gel Consistency

The test was based on the consistency of milled rice powder gelatinized by boiling in a diluted base and then cooled to room temperature [26]. To determine the gel consistency, 100 mg of milled rice flour was mixed with 2.0 mL of 0.2 N KOH in a test tube. The consistency was measured along the cold gel in 13 × 100 mm test tubes, which were held horizontally for 30–60 min. The gel consistency was classified as follows: hard (26–40 mm), medium (41–60 mm), and soft (61–100 mm).

2.4.5. Optimum Cooking Time

The optimum cooking time was determined using a standard method in which 2 g of milled rice was placed in a 100 mL beaker and boiled in 20 mL of water at 95 °C in a water bath [27]. The optimal cooking time was determined by pressing cooked rice samples between two glass dishes at regular intervals until no white starch core remained.

2.4.6. Water Uptake Ratio

The water uptake ratio was determined according to Bhattacharya and Sowbhagya [28]. An amount of 2 g of rice samples were boiled in 20 mL of water in a boiling water bath at 95 °C for the optimal cooking time. The remaining water was drained, and the cooked rice was transferred to a filter paper to absorb the surface water. The boiled samples were accurately weighed to calculate the water absorption ratio (WUR):

$$\text{WUR} = \frac{\text{Wt. of kernel after cooking (gm)}}{\text{Wt. of kernel before cooking (gm)}}$$

2.5. Grain Appearance and Textural Quality

2.5.1. Grain Length and Breadth

Nine rice grains were randomly selected to measure their length (mm) and width (mm) using a digital vernier caliper with the smallest number of 0.01 mm (Table S1). The grains were classified based on length as extra-long (>7.5 mm), long (6.61–7.5 mm), medium (5.51–6.60 mm), and short according to the classification given by IRRI.

2.5.2. Grain Shape

The shape of the grain was determined by the length-to-width ratio, which was calculated using the following equation before the husk was removed:

$$\text{Grain shape} = \frac{\text{Length (mm)}}{\text{Width (mm)}}$$

2.5.3. Kernel Shape

Kernel shape was determined by the length-to-width ratio, which was calculated using the following equation after the husk was removed:

$$\text{Kernel shape} = \frac{\text{Length (mm)}}{\text{Width (mm)}}$$

2.5.4. Husk Shape

The husk shape was estimated using the ratio of grain shape to kernel shape, calculated using the following equation:

$$\text{Husk Shape} = \frac{\text{Grain shape}}{\text{Kernel shape}}$$

2.5.5. Bulk Density

The bulk density (g/cm^3) of milled rice was calculated according to the equation used by Fraser et al. [29]:

$$\text{Bulk Density} = \frac{\text{Mass of rice (gm)}}{\text{Volume of vessel 100 mL}}$$

2.6. Expression Analysis of Genes Related to Amylose and Amylopectin Synthesis in Rice Genotypes

2.6.1. Collection of Leaf Samples

Leaf samples of rice cultivars were collected 25 days after sowing at IGKV, Raipur. A total of 9 samples were collected from each of the 9 genotypes. After collection, samples were wrapped in aluminum foil and immediately stored at liquid nitrogen (−196 °C) for total RNA extraction using Trizol reagent (protocol established at IOWA State University, Ames, IA, USA).

2.6.2. RNA Isolation and cDNA Preparation

Total RNA isolation was performed by the Trizol method established at Iowa State University, Iowa, starting by crushing the collected plant leaf into a fine powder in liquid nitrogen using a pestle and mortar. The resulting powder was then transferred to 2 mL tubes up to the 500 µL mark. Trizol reagent (500 µL) was added, followed by 10 min incubation at room temperature. A chloroform–isoamyl alcohol solution (24:1 v/v, 200 µL) was mixed into the lysate, incubated for 10 min, and centrifuged at 14,000 rpm for 15 min at 4 °C. The aqueous phase was transferred to a fresh tube, 500 µL ice-cold isopropanol

was added, and it was incubated for 10 min at room temperature to precipitate RNA. After centrifugation (14,000 rpm, 15 min, 4 °C), the pellet was washed with 500 µL DEPC-treated 70% ethanol, air-dried, and resuspended in 20 µL RNase-free DEPC water. The isolated RNA was quantified and used for cDNA synthesis using the Bio-Rad iScript cDNA Synthesis Kit (Bio-Rad, Hercules, CA, USA, catalog no. 1708891).

2.6.3. Semi-Quantitative RT-PCR

The expression of starch synthesis genes was analyzed by semi-quantitative reverse transcription polymerase chain reaction (semi-quantitative qRT-PCR). cDNAs synthesized from RNA extracted from fresh leaf samples of 9 rice genotypes were used for the expression analysis of nine different genes responsible for starch biosynthesis (Table 1). A semi-quantitative expression profile of the cDNA synthesized in the previous step was amplified using these gene-specific primers (Table S2). The PCR products were separated on a 1.25% agarose gel at 70 V. The presence and intensity of amplicons were recorded using a gel documentation system. Gene expression levels were determined based on the relative intensity of the amplicons and categorized as high, moderate, low, or insignificant.

Table 1. Functional classification of starch biosynthesis-related genes analyzed for expression profiling in rice genotypes.

Gene Name	Locus ID	Chromosome No	Tissue/Stage	Gene Function	Reference
OsSSIIb/SSII-2	Os02g0744700	2	Leaf	Elongation of α-glucan chains during amylopectin synthesis.	[9]
OsSSIIc/SSII-3	Os10g0437600	10	Endosperm	Elongation of α-glucan chains during amylopectin synthesis.	[30]
OsBt1	Os02g0202400	2	Endosperm	Transport of ADPG as *OsBT1*-ADPG complex from cytoplasm to amyloplast in endosperm	[31]
OsSBEIIa/SBE4	Os04g0409200	4	Leaf	An enzyme that acts on glycan induces branches connected by α-1, 6-glycosidic bonds.	[32]
OsISA1	Os08g0520900	8	Endosperm	*ISA1*, *ISA3* hydrolyze α-1, 6-glucosidic bonds and correct errors in starch synthesis to ensure regular amylopectin synthesis.	[33]
OsISA3	Os09g0469400	9	Leaf		[34]
OsGBP	Os02g0135900	2	Leaf	*OsGBP* and *OsFLO6*, homologues to *PTST1*, interact with *GBSSI* for its localization on surface of starch granules to drive amylose synthesis after phosphorylation.	[35]
OsFLO6	Os03g0686900	3	Grain/leaf		[36]

2.7. Analysis of Genetic Variability for Starch Biosynthesis-Related Genes and Identification of Alleles for Low and High Amylose Content

To study the genetic variation among selected rice genotypes, the process began with retrieving the International Rice Research Institute (IRRI) accession IDs for the chosen genotypes. Subsequently, the SNP-Seek database (snp-seek.irri.org) was accessed to create a list of the selected varieties. Once the variety list was created, the chromosome number corresponding to the gene of interest was specified for genetic variation analysis. The locus ID of the gene was then entered, or alternatively, the chromosomal region encompassing the gene was defined by specifying the start and end positions. After entering this information, the analysis was executed to assess genetic variation. Additionally, alleles were organized into the required number of groups to enable a comprehensive interpretation of the results. By following these steps, genetic variations were effectively analyzed, and allelic variations were classified into specific groups (Figure 2).

2.8. Statistical Analysis

Statistical analysis was performed using the online tool OpStat PythonAnywhere (http://opstat.pythonanywhere.com, accessed on 2 July 2025) to conduct descriptive statistical analysis. R packages v.4.1.2 were used to create a Pearson correlation heat map, which provided a visual representation of the relationships between variables in the dataset. Bar graphs were generated using Microsoft Office Professional Plus 2021, Excel version 2108.

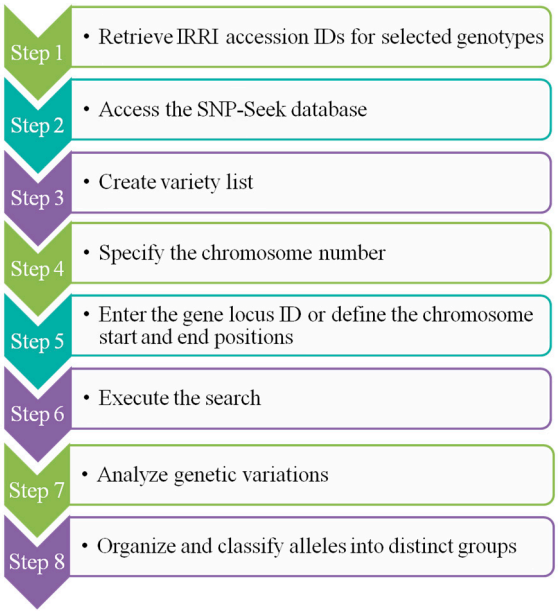

Figure 2. Workflow for study of sequence variation among the starch biosynthesis genes in different genotypes using the SNP-Seek database.

3. Results

3.1. Starch Granule Size and Morphology

The results of SEM (scanning electron microscopy) analysis of starch granule (SG) morphology, among the investigated rice genotypes, showed significant differences in size, shape, and arrangement of SG in 2D and 3D space (Figure 3). Notably, the genotype NON-HAI exhibited the largest granule surface area (47.68 μm^2), while Hap 3-3 P-11 had the smallest (20.06 μm^2). Other genotypes showed intermediate values, with SG size ranging from 23.22 μm^2 for IRRI 147 to 35.65 μm^2 for Makro (Table 2). A negative correlation (−0.73) was obtained between SG surface area and amylose content (AC), while glycemic index (pGI) and SG surface area were positively correlated (0.76). Correlation of larger SG surface area with higher pGI showed these grains had lesser resistance starch (Figure 4). Additionally, the circularity and SG in the 2D interface, along with morphology in the 3D surface plot, were analyzed for each genotype (Table 2). The 3D visualization provided a detailed comparison of surface samples, highlighting differences in shape, texture, and roughness (Table 3). Unique structural features, ranging from high roughness with pronounced peaks and valleys to smoother surfaces with gentle undulations, were observed in each sample (Figure 5). The 2D analysis of the starch surface perimeter revealed that IRRI 147 had the highest circularity value (0.883), indicating that it had the most spherical starch granules among all the genotypes. In contrast, Makro showed the lowest circularity at 0.809, suggesting a less circular granule shape or more polygonal structures. The circularity values of the other genotypes ranged from 0.827 for Hap 3-3 P-11 to 0.859 for Swarna, reflecting a spectrum of granule shapes across the different rice genotypes (Table 2).

Although the surface smoothness or shape of the SG was not directly correlated to the pGI value, they had an impact on organoleptic properties. Grains with irregular polygonal shapes (Makro, Hap 3-3 P-11, Hap 3-1 P-22, and Hap 3-1 P-18) had hard grain texture. The genotypes like Amber, Swarna, and M-55 were spherical SGs with smooth surfaces, whereas the genotypes NON-HAI and IRRI-147 showed a mixture of both spherical and irregular or polygonal shapes.

Table 2. Comparative analysis of starch granule morphology, biochemical properties, and physicochemical traits across nine rice genotypes.

S.N.	Genotypes	SG Surface Area (μm^2)	SG Perimeter (μm)	Amylose Content (%)	Total Starch (%)	pGI	Starch Shape (Circularity)	Gel Consistency (mm)	Water Uptake Ratio	Optimum Cooking Time (min)	Bulk Density (kg/m^3)
1	IRRI 147	23.22	18.15	30.8	76.36	56.2	0.88	56	3.09	47	566.63
2	NON-HAI	47.67	26.61	6.39	82.95	82.46	0.85	95	3.11	50	504.77
3	Amber	34.09	22.46	31.5	78.78	63.97	0.84	34	3.53	46	435.15
4	Swarna	33.09	21.97	29.6	65.84	58.06	0.86	30	3.49	46	516.97
5	Makro	35.64	23.58	30.6	71.88	59.06	0.80	91	3.22	47	561.70
6	Hap 3-3 P-11	20.05	17.46	32.8	81.7	41.07	0.82	42	3.62	44	587.50
7	Hap 3-1 P-22	34.29	22.40	36.9	84.11	42.34	0.85	19	3.22	42	601.63
8	Hap 3-1 P-18	27.46	20.06	33.1	75.34	41.79	0.85	24	3.42	51	531.27
9	M-55	26.27	19.70	32.7	83.68	54.42	0.85	71	3.11	48	583.44
	Mean $\pm$ SD	31.31 $\pm$ 8.20	21.38 $\pm$ 2.85	29.38 $\pm$ 8.87	77.85 $\pm$ 6.15	55.49 $\pm$ 13.17	0.85 $\pm$ 0.02	51.33 $\pm$ 28.55	3.32 $\pm$ 0.20	46.78 $\pm$ 2.77	543.23 $\pm$ 52.28

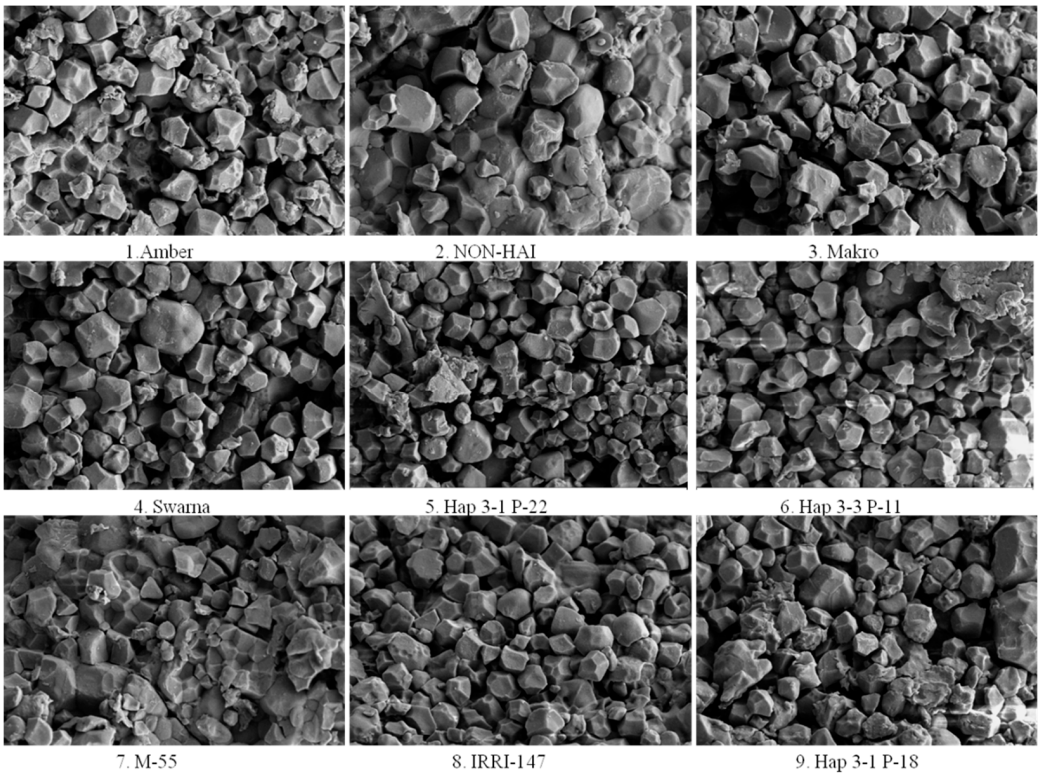

Figure 3. Scanning electron microscopy (SEM) images of starch granules of nine investigated rice genotypes.

Table 3. Interpretation of starch granule morphology and surface texture across different rice genotypes of 3D imaging results.

Genotypes	Shape Description	Texture Description	Implications
Amber	The starch granules exhibit predominantly spherical shapes with a high degree of uniformity. The granules are well-rounded, indicating consistent starch biosynthesis.	The surface is smooth with minimal irregularities. There are few to no indentations or protrusions, suggesting a stable and uninterrupted formation process.	The uniform shape and smooth texture may contribute to predictable gelatinization properties, making Amber suitable for products requiring consistent texture and viscosity.
NON -HAI	Granules are primarily oval to slightly elongated. Some granules display minor angularity, indicating variability in granule development.	The surface texture is moderately smooth with subtle ridges. These slight variations may reflect differences in amylopectin branching during starch synthesis.	The moderate smoothness and shape variability might affect the granules' packing, impacting the texture of the final product.
Makro	The granules are irregularly polygonal, with a mix of spherical and angular forms. This diversity suggests heterogeneous biosynthetic activity.	Surfaces exhibit mild roughness with noticeable facets and edges. The textural variation may affect the granules' packing and interaction.	The diverse shapes and textures may influence water absorption rates and gelatinization behavior during cooking.
Swarna	Starch granules are predominantly spherical with occasional oval forms. There is also noticeable elongation in some granules, deviating from typical spherical forms.	The surface is smooth with minimal textural deviations. A consistent surface suggests efficient starch synthesis enzymes.	The overall uniformity indicates coordinated starch deposition.
Hap 3-1 P-22	Granules display irregular and elongated shapes, with some appearing rod-like or kidney-shaped. This irregularity hints at genetic variations affecting granule formation.	The surface is rough with pronounced grooves and depressions. These features indicate disruptions or alterations in the starch layering process.	The rough texture and irregular shape may alter gelatinization properties and enzymatic digestibility, affecting cooking quality and nutritional aspects.
Hap 3-3 P-11	The starch granules are highly irregular, with fragmented and angular shapes dominating the sample. Such variability suggests significant genetic divergence.	Surfaces are very rough with sharp edges and pronounced irregularities. This roughness may be due to aberrant starch synthesis or environmental stress during development.	Such granules may behave differently during processing, impacting texture and consistency in food applications.

Table 3. *Cont.*

Genotypes	Shape Description	Texture Description	Implications
M-55	Starch granules are predominantly spherical with some oval forms. They are uniform in size, indicating coordinated biosynthesis.	The surface is smooth with slight undulations. Minor surface variations hint at standard starch synthesis with minimal disruptions.	The consistent shape and texture are favorable for applications requiring predictable starch behavior, such as in baking or thickening agents.
IRRI-147	Exhibits a mix of spherical and polygonal granule shapes. Some granules have well-defined edges, while others are more rounded.	The surface is moderately rough, featuring small ridges and facets. Variability may reflect differences in enzyme activities during starch formation.	This genotype may offer unique textural properties suitable for specialized culinary uses or industrial applications.
Hap 3-1 P-18	Primarily spherical granules with some irregularities in shape. There is a mix of sizes, suggesting a heterogeneous granule population.	The surface is rougher compared with other genotypes, with noticeable grooves and indentations. Indicates potential genetic factors affecting surface morphology.	The rough texture may enhance enzymatic access, possibly improving the digestibility of starch and influencing the glycemic index.

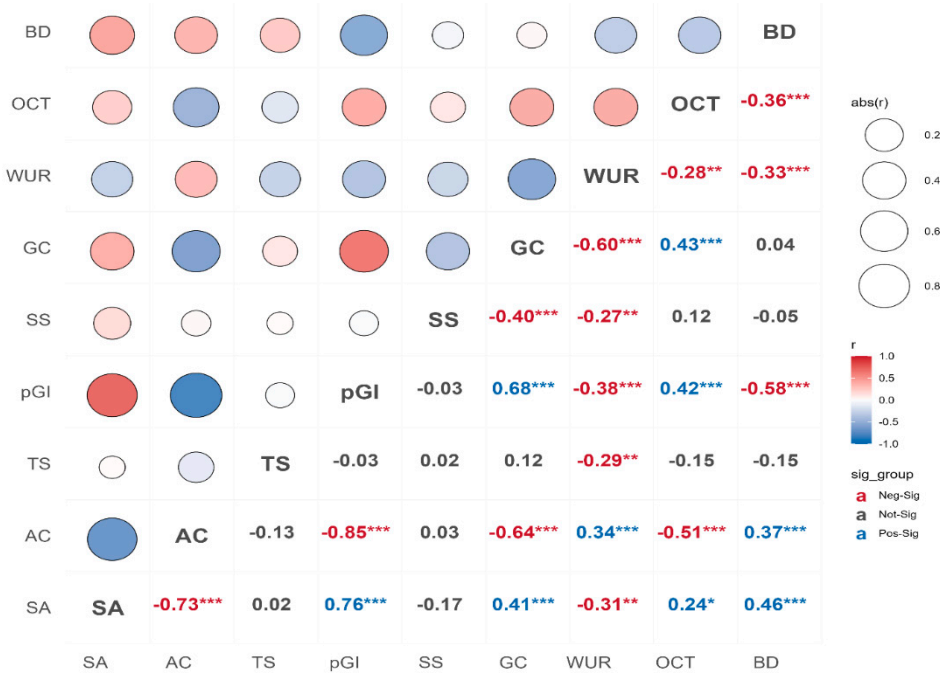

Figure 4. Correlation coefficient investigation shows the associations among starch granule size, amylose content, and glycemic index, with other physicochemical traits in rice. SA—starch granule surface area; AC—amylose content; TS—total starch; pGI—predicted glycemic index; SS—starch shape; GC—gel consistency; WUR—water uptake ratio; OCT—optimum cooking time; and BD—bulk density. * Significance at p-value < 0.05. ** Significance at p-value < 0.01. *** Highly significant at $p < 0.001$. abs(r)—absolute correlation (bubble sizes in the heat map represent absolute correlation strength ($|r|$), where larger bubbles indicate stronger linear associations).

3.2. Amylose Content, Total Starch, and Glycemic Index

The amylose content among nine rice genotypes ranged from 6.93% in NON-HAI to a maximum 36.9% in Hap 3-1 P-22 (Table 2). The AC was found to be negatively correlated (−0.85) with pGI. The M-55 variety with 32.7% AC had a pGI value of 54.82, whereas the genotypes Hap 3-3 P-11 and Hap 3-1 P-18 with 32.8% and 33.1% AC showed a pGI around 41. The difference in pGI could be explained by irregular polygonal SGs with rough surfaces found in Hap 3-3 P-11 and Hap 3-1 P-18, whereas the SGs of M-55 were more spherical with smooth surfaces. These results indicate the scope of the development of low-pGI rice with intermediate AC by bringing change to the SG structures and packing in grains.

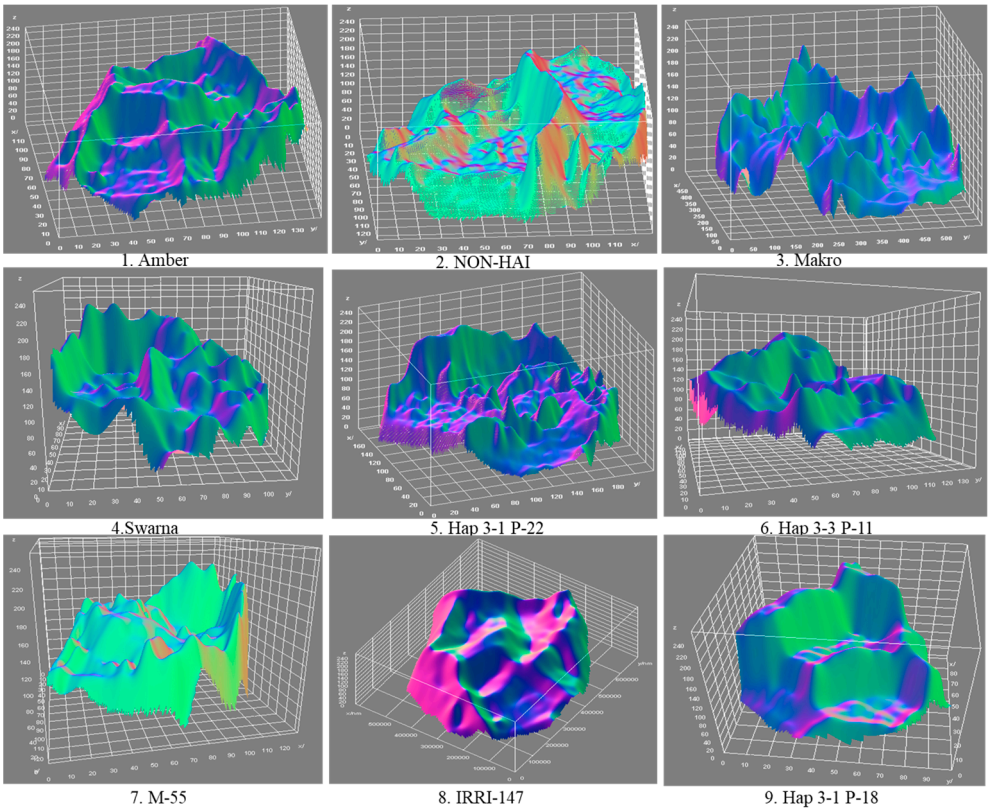

Figure 5. Three-dimensional (3D) surface plot of starch granules, illustrating morphological diversity of starch granules in selected rice genotypes (Source: Generated using imagej.net).

Further, our study of pGI on selected rice genotypes showed that the lines (Hap 3-3 P-11, Hap 3-1 P-22, and Hap 3-1 P-18) developed via Swarna × Aus 329 cross had low pGI, which was around 41. In contrast, NOH HAI has the highest pGI (82.46), while established varieties (IRRI-147, Swarna, Makro, and M-55) showed intermediate pGI values (~56). Additionally, a negative correlation between amylose content and pGI suggested that higher amylose levels may contribute to a lower glycemic response. Total starch content varied substantially among genotypes, ranging from 65.84% (Swarna) to 84.11% (Hap 3-1 P-22), with a mean of 77.46%. Hap 3-1 P-22 exhibited the highest starch content (84.11%), followed by M-55 (83.68%) and Hap 3-3 P-11 (81.70%). Conversely, Swarna exhibited the lowest total starch content (65.84%). Genotypes with moderate total starch content (70–80%) included Amber (78.78%), Makro (76.42%), Hap 3-1 P-18 (71.88%), and IRRI 147 (76.36%).

3.3. Gel Consistency, Optimum Cooking Time, and Water Uptake Ratio

Larger starch granules (e.g., NON-HAI: 47.68 μm^2 surface area) correlated with softer gels (95 mm) and longer cooking times (50 min), while smaller granules (e.g., Hap 3-3 P-11: 20.06 μm^2) associated with harder gels (42 mm) and shorter cooking times (44 min) (Table 2). This pattern aligned with a negative correlation between amylose content and granule size. Starch shape showed weaker trends where elongated granules (e.g., NON-HAI) trended toward softer gels but showed inconsistent cooking times, while spherical granules (e.g., Amber: 34 mm gel) typically formed harder gels unless amylose was low (e.g., M-55: 71 mm gel). Notable exceptions, i.e., Hap 3-1 P-18 (small granules, 51 min cooking time), suggested that amylose content could override morphological influences. Water uptake (42–51 min) showed no clear dependency on size or shape, implying roles for porosity or chemical composition (Table 2). Overall, granule size and amylose content dominated functional predictions, while shape offered secondary insights.

3.4. Physio-Morphology of Rice Grains

Genotypic variation in rice grain physiology aligned with prior studies. Grain length before husk removal ranged from 6.65–9.63 mm, with Amber (9.63 mm) and NON HAI (6.65 mm) representing the longest and shortest grains, respectively, while most of the genotypes (e.g., Makro, Hap 3-1 P-18/P-22: 7.5–8.5 mm) had intermediate ranges (Figure 6). Grain width with husk varied from 2.33 mm (Hap 3-3 P-11) to 3.18 mm (M-55), with moderate values in Amber (2.64 mm) and Swarna (2.47 mm). The length-to-width (L/W) ratio, critical for cooking quality, texture, and market preference, ranged from 2.4 to 3.7. Amber (L/W = 3.64) and Hap 3-1 P-22 (L/W = 3.28) exhibited the most elongated grains, contrasting with IRRI 147 (L/W = 2.437) and M-55 (L/W = 2.46), which displayed rounded grains (Figure 6). After removing the husk, the highest and lowest lengths were observed in Amber (6.92 mm) and Hap 3-3 P-11 (5.14 mm), respectively, and for width, the highest and lowest values were observed in M-55 (2.78 mm) and Hap 3-3 P-11 (2.07 mm), respectively. Here the trend of highest and lowest values of width for both with husk and without husk and, similarly, the highest value of length for both with husk and without husk remained the same, but the lowest value for length was shifted from NON-HAI to Hap 3-3 P-11; to understand this shift, we should have a better understanding of husk shape. The husk shape ratio (grain shape/kernel shape) provided insights into structural traits affecting milling efficiency. Makro had the highest ratio (1.306), indicating favorable hull removal, while NON-HAI showed the lowest (1.08), and most of the genotypes had husk shape ratios between 1.25 and 1.28 (Figure 6). NON-HAI had the lowest husk shape ratio, even though it was the shortest grain length with husk and but not in the case of without husk.

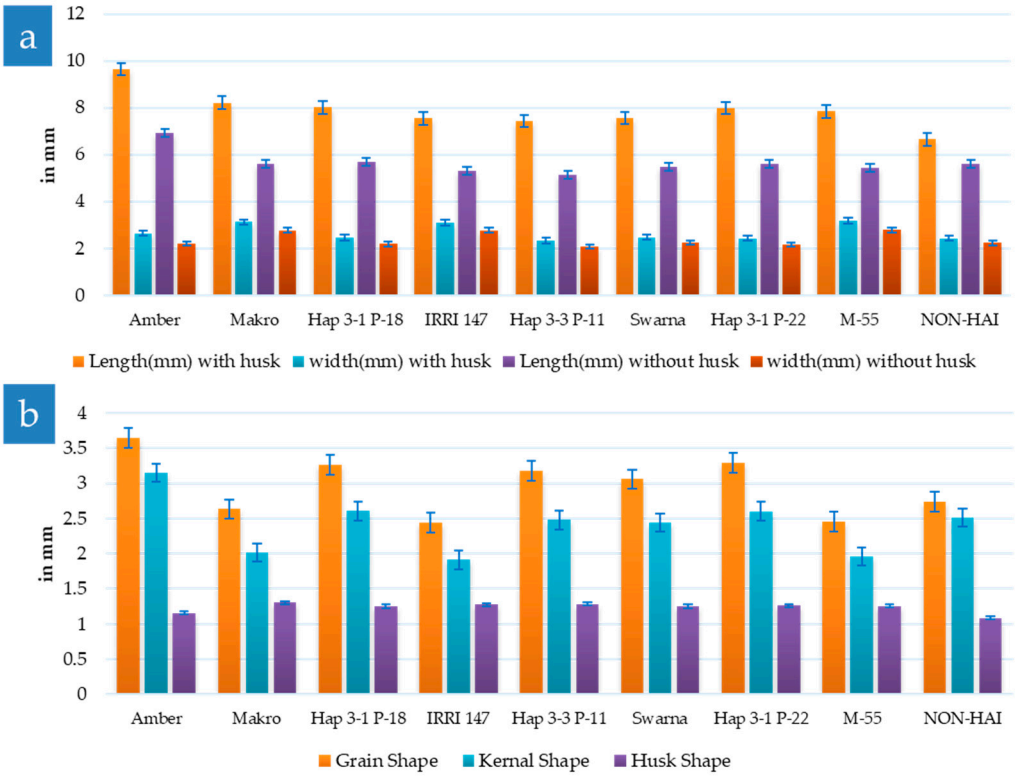

Figure 6. Morphological characterization of rice grains: (**a**) grain length and width before and after removing husk and (**b**) grain shape, husk shape, and kernel shape.

3.5. Expression Analysis of Genes Related to Amylose and Amylopectin Synthesis

The expression of *OsBt1*, *OsSSIIb*, *OsSSIIc*, *OsSBEIIa*, *OsGBP*, *OsFLO6*, *OsISA1*, and *OsISA3* genes was analyzed in the leaf tissue of 25-day-old rice genotypes, and for normalization, the housekeeping gene actin was used (Figure 7) (Table S3). The analysis of starch

biosynthesis genes across nine rice genotypes revealed distinct regulatory patterns with significant implications for starch functionality. Key genes involved in amylopectin synthesis, such as *OsSSIIb* and *OsSSIIc*, responsible for elongating α-1, 4-glucan chains, predominantly showed higher levels of expression across the genotypes, except for *OsSSIIc* in Hap 3-1 P-22, promoting longer, more linear amylopectin chains. This elongation enhanced starch crystallinity, likely elevating gelatinization temperatures and yielding firmer gels, as seen in genotypes like NON-HAI (gel length = 95 mm) and M-55 (gel length = 71 mm), while in Hap 3-1 P-22, *OsSSIIc* showed a low level of expression, which also further correlated with a shorter gel length of 19 mm (the lowest in our result) (Table 2). Conversely, *OsSBEIIa*, which introduced α-1, 6-branches, was low in expression in all genotypes. The higher level of expression for *OsBt1*, critical for transporting ADP-glucose into amyloplasts, indicated heightened substrate availability, bolstering overall starch accumulation. Amylose synthesis was notably influenced by *OsGBP* and *OsFLO6*, which facilitated starch localization with *GBSSI*. *OsFLO6* showed a lower level of expression across all genotypes, while *OsGBP* showed a higher level of expression, except it showed no expression in IRRI-147, which was the low GI rice line. The lower level of expression of *OsISA3* across all genotypes depicted a comparative pivotal role of *OsISA1* toward starch granule morphology.

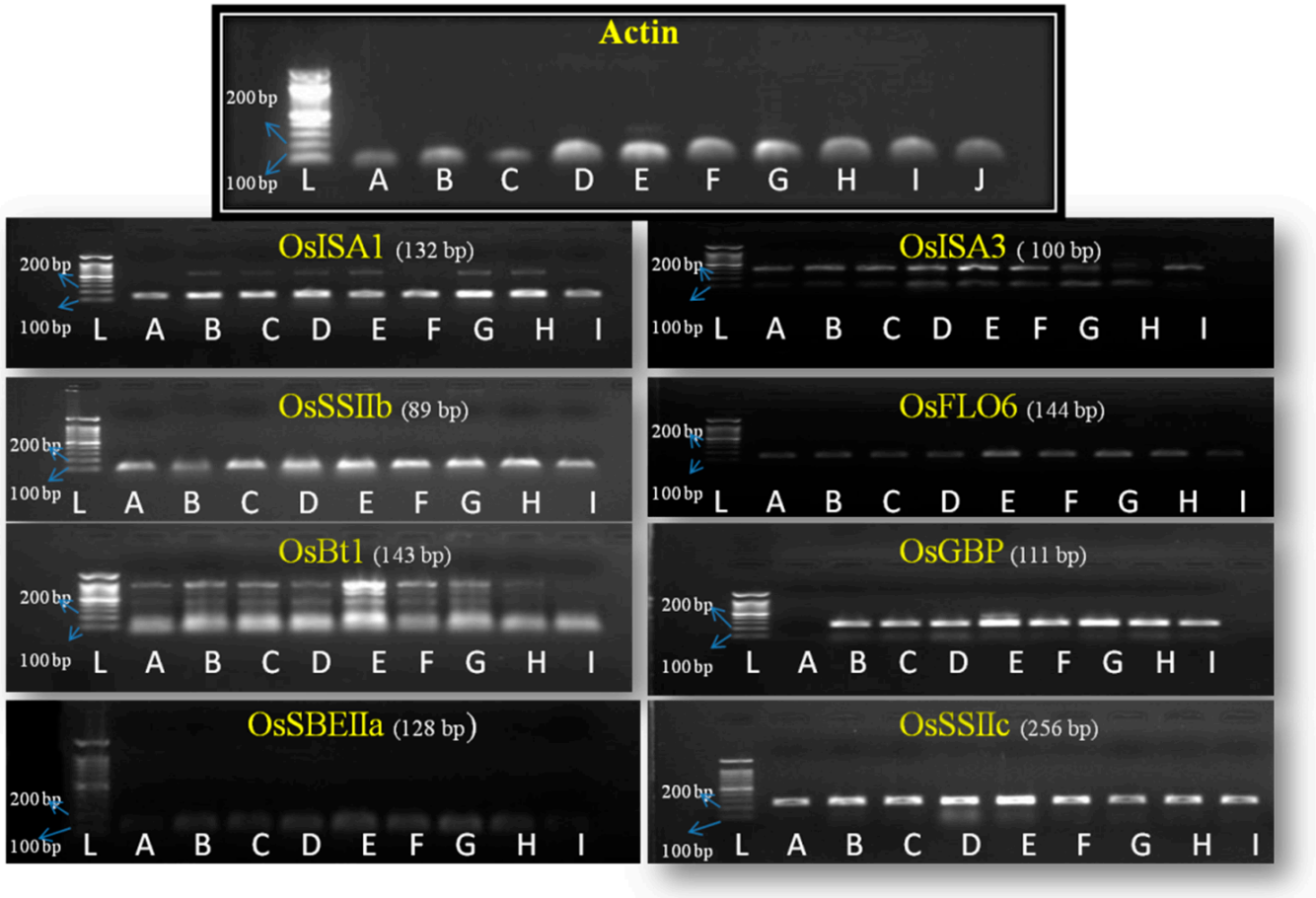

Figure 7. Semi-quantitative RT-PCR expression patterns of starch biosynthesis-related genes in different rice genotypes, where L = Ladder (100 bp), A = IRRI-147, B = NON-HAI, C = Amber, D = Swarna, E = Makro, F = Hap 3-3 P-11, G = Hap 3-1 P-22, H = Hap 3-1 P-18, I = M-55, and J = control.

3.6. Genetic Variability and Identification of Allele

To investigate the association between genetic variation in eight key starch biosynthesis genes (*OsBt1*, *OsSSIIb*, *OsSSIIc*, *OsSBEIIa*, *OsGBP*, *OsFLO6*, *OsISA1*, and *OsISA3*) and

amylose content (AC), 20 diverse rice genotypes were selected from the Rice3K SNP-seek database panel based on their AC levels, as previously analyzed in a set of 250 genotypes in our laboratory (Table 4) [37]. Genetic variation analysis revealed no significant association between allele groups and AC for most genes, except for *OsGBP* (Table S4). Notably, *OsGBP* allelic variants showed clear associations with AC, where allele group 2 was associated with significantly reduced AC (9.62%) (Table 5), while all other allele groups maintained consistently high AC levels (22–24%) (Table S5). This finding highlights the potential role of *OsGBP* in regulating amylose content, which may further influence glycemic index (GI) and starch functionality.

Table 4. Selected genotypes from the 3K panel were used for studying allelic variation.

S.N.	Genotypes	Accession ID	Amylose % 2020	Amylose % 2021	Mean
1	NOROI	IRGC 121069	24.34	27.91	26.12
2	SOLOMON RED RICE	IRGC 126312	27.12	30.09	28.60
3	GOKAUNG	IRGC 128045	21.86	30.06	25.96
4	IR 3839-1	IRGC 127437	23.87	29.62	26.74
5	JIN JUN DAO	IRGC 125613	27.02	28.68	27.85
6	NCS 237	IRGC 125853	23.43	28.51	25.97
7	IR 4432-28-5	IRGC 127438	30.20	27.81	29.01
8	CHAKOL	IRGC 125696	25.61	28.28	26.95
9	IR 77390-1-6-4-19-1-B	IRGC 127075	17.50	28.04	22.77
10	IRRIBINI	IRGC 126215	30.21	28.01	29.11
11	BENGALY MORIMO	IRGC 125677	25.31	21.61	23.46
12	IRI 339	IRGC 125778	20.42	21.51	20.96
13	IRGA 659-1-2-2-2	IRGC 120993	15.09	17.35	16.22
14	ARC 12576	IRGC 125645	12.27	17.15	14.71
15	RD 15	IRGC 126003	13.45	16.55	15.00
16	ARC 11901	IRGC 127033	18.54	15.95	17.24
17	KHAO DAWK MALI 105	IRGC 121235	7.48	10.55	9.02
18	ARC 13778	IRGC 125647	5.54	9.31	7.42
19	KAM PAI	IRGC 126152	4.80	9.14	6.97
20	NEP BA BONG TO	IRGC 128116	6.01	9.01	7.51

Table 5. Allelic variations in the *OsGBP* gene, which are associated with low AC.

K-GROUP	Variety	Amylose Content	chr02-1909569	chr02-1909678	chr02-1909917	chr02-1910147	chr02-1910189	chr02-1910611	chr02-1910815	chr02-1910818	chr02-1911075	chr02-1911438	chr02-1911890	chr02-1912215	chr02-1912277
2	NEP BA BONG TO::IRGC 17005-2 RD 15::IRGC 47705-1 KHAO DAWK MALI 105::IRGC 27748-2 KAM PAI::IRGC 78245-1	9.62	C	A	A	A	G	C	T	G	T	C	C	T	C

4. Discussion

Our research revealed a significant negative correlation between the surface area of starch granules and amylose content, as well as a strong positive correlation between starch surface area and glycemic index, aligning with the findings of Ramadoss et al. [38]. Although higher AC ensures lower pGI, it also brings negative traits like hard and chewy grains upon cooking. In this study, we focused on the identification of cooking and eating quality-related traits that varied in genotypes with similar AC. Apart from the relative proportion of amylose and amylpectin, pGI is also determined by other factors such as molecular structure, as well as the physicochemical properties of the starch, size, and shape of the starch granules. The structure of rice starch granules affects its digestibility in vitro. Previous reports on the correlation of starch granule size and structure with in vitro digestibility indicate that rice genotypes with similar amylose content may have different pGI values [39]. Previous reports on cereals such as wheat and maize have indicated that superior and inferior grain quality (cooking and gelatinization properties) are associated with the size of starch granules [40]. Zhao et al. showed that the shape, along with the size, of starch granules influenced grain starch quality, where starch granules from superior grains were polygonal in shape and larger [41]. In our study also, electron microscopy of the SG in rice genotypes with similar AC showed variation in the size, shape, and compactness of the grain. The properties of SG (size and surface area) were found to be positively correlated to pGI and gel consistency. The SG with spherical shape and uniform surfaces were observed in Swarna and M55, which had compact grains with higher bulk density, while the grains with irregular (polygonal/angular) starch grains having rough surfaces belonged to the ones (Makro, Hap 3-3 P-11, Hap 3-1 P-22, Hap 3-1 P-18, and NOH HAI) that had lower bulk density. All these genotypes had varying AC, such as 6.89% in NOH HAI, whereas Makro, Hap 3-3 P-11, Hap 3-1 P-22, and Hap 3-1 P-18 had an average AC of 33.35%. Negative correlation (−0.58) was observed between bulk density and pGI, and the same has been reported by other researchers [42]. These results indicate that there is a possibility to create a genetic combination where the genotypes have slightly higher AC (~26–28%). We can obtain intermediate pGI values by bringing the desired changes in the size, shape, and packaging of SG in rice grains. The observations recorded in genotypes IRRI147, which showed 30.6% AC and lower pGI (56.2), and M55, with AC (32.7%) and pGI (54.42), supported our hypothesis. A recent report on the development of low and intermediate GI lines showed decreased amylose content based on soluble dietary fiber content and starch properties [43]. We also found that the genotype IRRI 147 had a mixture of spherical-uniform and irregular-polygonal SGs, whereas the genotype M-55 had small, smooth, spherical SGs. These findings implied that with variations in the size and shape of SGs, the value of lower pGI could be achieved even in the lines with higher AC or vice versa. Analysis of starch granules in rice has not been conducted as extensively at the molecular level, which can lead to identification of potential candidate genes for developing rice varieties with lower GI and still better organoleptic properties. SG size and shape are known to influence the overall surface area, which in turn influences enzyme accessibility. Singh et al. have reported that rapid hydrolysis of starch is facilitated by increased enzyme accessibility owing to the larger surface area of SGs [5]. Thus, strategically modifying the characteristics of starch granules could be an effective strategy for enhancing the quality and nutritional profile of rice.

We observed a negative correlation between amylose content and pGI, which aligns with previously established research demonstrating that rice varieties with higher amylose content tend to have a lower pGI [14,15]. Amylose, a linear and less digestible starch component, influences the overall digestibility of rice. Varieties with higher amylose content may undergo slower starch breakdown during digestion, resulting in a more gradual rise in

blood sugar levels and a potentially lower pGI. Additionally, the lower total starch content might contribute to a distinct compositional profile and potentially cater to specific market preferences for rice with different energy content. Meanwhile, a moderate starch range could provide an optimal balance between energy content and structural characteristics, enhancing the versatility of these varieties for diverse culinary applications [5,44].

A high pGI is associated with a rapid increase in blood sugar levels, making such varieties less suitable for individuals with diabetes or those following a low-pGI diet [45]. Conversely, rice varieties with a low pGI, such as Hap 3-1 P-18, Hap 3-3 P-11, and Hap 3-1 P-22 (41.79, 41.07, and 42.34, respectively), may be more suitable for diabetic individuals due to their potential for a slower rise in blood sugar levels [46]. The observed negative correlation between amylose content (AC) and pGI aligns with previous research, further supporting the idea that rice varieties with higher amylose content tend to exhibit lower pGI values; however, the relationship is not linear.

Variations in cooking time have important implications in determining the method of cooking and consumer preference. Genotypes with longer cooking times, such as Hap 3-1 P-18 (51 min) and M-55 (48 min), are well suited for firmer textures in dishes like pilaf. Conversely, varieties such as Amber, Makro, IRRI 147, and Swarna (cooking times of 46–47 min) provide a desirable balance between firmness and tenderness. Notably, Hap 3-3 P-11 and Hap 3-1 P-22 cooked faster (44 and 42 min, respectively), indicating their suitability for quick-cooking dishes. A moderate positive correlation was found between cooking time, pGI, and gel consistency, suggesting interconnections that merit further research [7,47,48].

The negative correlation (−0.60) between the water uptake ratio (WUR) and the gel consistency indicates that rice with a higher WUR may have a less dense gel network, resulting in lower gel consistency. This is likely due to greater water absorption disrupting gel formation. Higher water uptake might also correlate with increased amylose leaching during cooking, further affecting gel consistency [49]. However, other factors, such as amylose content and starch granule size, also influence gel consistency and warrant further investigation.

The observed genotypic variation in rice grain physiology, as detailed in the study, aligns with previous research, emphasizing the significant influence of genetic traits on grain quality and processing efficiency. Grain lengths before husk removal ranged from 6.65 to 9.63 mm, and width varied from 2.42 mm (Hap 3-3 P-22) to 3.18 mm (M-55). After removing the husk, the highest and lowest lengths were observed in Amber (6.92 mm) and Hap 3-3 P-11 (5.14 mm), respectively, and for width, the highest and lowest values were observed in M-55 (2.78 mm) and Hap 3-3 P-11 (2.07 mm), respectively. Here the trend of highest and lowest values of width for both with husk and without husk and, similarly, the highest value of length for both with husk and without husk remained the same, but the lowest value for length was shifted from NON-HAI to Hap 3-3 P-11, and to understand this shift, we should have a better understanding of husk shape. The husk shape ratio (grain shape/kernel shape) result showed that NON HAI had the lowest value (1.08), so even though it was shown as having the shortest length with husk, it was not the case without husk. The length-to-width (L/W) ratio, a key factor influencing cooking quality and texture, ranged from 2.3 to 3.7, with elongated grains like Amber (3.64) and Hap 3-1 P-22 (3.28) associated with superior cooking and organoleptic properties, such as desirable texture and elongation [50]. In contrast, rounder grains like IRRI 147 (2.43) and M-55 (2.46) were linked to shorter cooking times and better water absorption, catering to specific culinary needs [51,52]. The husk shape ratio, which impacts milling efficiency, further revealed variability, with Makro (1.30) showing favorable hull removal traits. These findings underscore the importance of genotypic traits in determining rice quality, milling

performance, and consumer appeal, emphasizing the potential for breeding programs to optimize grain characteristics for improved processing efficiency and marketability [52].

The gene expression analysis suggested that the absence or disruption of *OsGBP* may contribute to a lower glycemic index (pGI), as observed in IRRI-147. Conversely, *OsSBEIIa*, which introduced α-1, 6-branches, was low in expression in all genotypes, suggesting fewer branch points and potentially reduced solubility and swelling power, which may lower paste viscosity and alter gelling behavior. In addition, debranching enzymes further refine starch structure; *OsISA1* higher expression in most genotypes ensured precise trimming of amylopectin, fostering compact granules with high bulk density. Exceptions like Makro, with downregulated *OsISA1*, may develop irregular, porous granules, which can also be seen in our SEM result, which is associated (Makro = irregularly polygonal). *OsISA1* consistently shows more upregulation than *OsISA3* in all rice genotypes. Since *OsISA3* plays a crucial role in starch initiation and morphology, its downregulation in most genotypes except in Amber, a high-pGI variety, indicated a possible link between *OsISA3* expression and increased pGI. We assumed that upregulated expression of *OsISA3* may significantly affect starch structure, which would be one reason for the increased pGI observed in Amber. The results of genetic variability for starch biosynthesis genes among various genotypes suggest that despite variations, certain alleles or allele groups are associated with higher amylose content. These findings provide valuable genetic markers that could be utilized in breeding programs to develop rice varieties with desirable starch composition and glycemic properties.

The genetic variability analysis indicated that specific alleles of certain genes were preferred for high amylose content in rice. Notably, the correlation between amylose content and the gene *OsGBP* was very surprising as although it was primarily responsible for starch packaging, it could still help modify the rice's glycemic index. So, by targeting such genes, we could modify GI without compromising key consumer-preferred grain characteristics.

Based on expression analysis, we found that *OsGBP* and *OsISA1* genes had roles in influencing glycemic index as they are known to play roles in starch packaging, influencing starch morphology. The allelic variation found at positions chr02-1909569 chr02-1909678, chr02-1909917, chr02-1910147, chr02-1910189, chr02-1910611, chr02-1910815, chr02-1910818, chr02-1911075, chr02-1911438, chr02-1911890, chr02-1912215, and chr02-1912277 in *OsGBP* was found to be associated with low amylose content. Thus, these genes may be used to modify the starch granule size and packaging in rice grains to achieve lower to intermediate GI without increasing the AC significantly. Further exploration of the variation in the nucleotide sequence of these genes will pave the way for CRISPR-mediated editing. Thus, these findings may inform future genome editing efforts aimed at reducing GI. Since these genes are involved in later steps of starch biosynthesis, therefore, the modifications of these genes will not lead to major disturbances in starch synthesis, which was an issue in earlier efforts. Previous studies on the genetic modification of starch biosynthesis-related major genes (*AGPase*, *GBSS*, *SBE*, and *SS*) have shown disturbance in normal starch synthesis, grain shape, and poor organoleptic properties. Thus, exploring these starch traits enhances our understanding of the complex relationship between starch morphology, amylose content, and glycemic index. This knowledge ultimately contributes to advancements in health, nutrition, and food stability.

5. Conclusions

In conclusion, the research showed significant correlations between starch surface area, amylose content (AC), and glycemic index (GI), emphasizing the significance of starch morphology in influencing glycemic index (GI). Our study found a negative correlation between starch granule surface area and amylose content, as well as a positive correlation

between starch surface area and glycemic index (GI). This suggests that breeders should consider factors such as starch initiation, morphology, and packaging genes like *OsGBP* and *OsISA* when developing low-GI rice varieties. The research also highlights the potential of *OsISA1* and *OsGBP* in modifying starch characteristics and amylose content, offering new insights for future rice breeding efforts.

Supplementary Materials: The following supporting information can be downloaded at: https://www.mdpi.com/article/10.3390/pr13103241/s1, Table S1: Morphological characterization of rice grains: (a) grain length and width before and after removing husk and (b) grain shape, husk shape, and kernel shape; Table S2: List of Primers used for gene expression study; Table S3: Actin normalization details to check gene expression; Table S4: Grouping of genotypes as per allele group to underscore the relation with amylose content; Table S5: Result of OsGBP allelic variation generated from using SNP-seek database.

Author Contributions: Conceptualization, S.B. and A.A.; methodology, S.B., A.A., S.S.R. and P.R.; software, S.B. and M.Q.; validation, S.B. and V.K.P.; formal analysis, S.B., A.A., M.Q. and S.S.R.; investigation, S.B., A.A. and V.K.P.; resources, S.B.; data curation, S.B., S.S.R., P.R., V.K.P. and T.B.; writing—original draft preparation, A.A. and P.R.; writing—review and editing, S.B., M.Q., M.N., N.D. and K.A.; visualization, S.B. and A.A.; supervision, S.B.; project administration, S.B. All authors have read and agreed to the published version of the manuscript.

Funding: Partial funding was provided by Indira Gandhi Krishi Vishwavidyalaya, Raipur, for article processing charges (APCs).

Data Availability Statement: The original contributions presented in this study are included in the article/Supplementary Materials. Further inquiries can be directed to the corresponding authors.

Acknowledgments: We thank the Department of Plant Molecular Biology and Biotechnology, Indira Gandhi Krishi Vishwavidyalaya, Raipur, for providing space and all basic facilities for conducting this research.

Conflicts of Interest: The authors declare no potential conflicts of interest concerning the research, authorship, and/or publication of this article.

Abbreviations

The following abbreviations are used in this manuscript:

GI	Glycemic index
pGI	Predicted glycemic index
AC	Amylose content
SG	Starch granule
GC	Gel consistency
OsSSIIb	Rice Starch Synthase IIb
OsGBP	Rice Granule-Binding Protein
OsFLO6	Rice Granule-Binding Protein FLO6
OsISA3	Rice Isoamylase 3
SSIIa	Starch Synthase IIa
SBE	Starch Branching Enzyme
SBEIIb	Starch Branching Enzyme IIb
OsBt1	Brittle 1
RS	Resistant starch
GBSSI (Wx)	Granule-Bound Starch Synthase I (Waxy Gene)
CRISPR	Clustered regularly interspaced short palindromic repeats
Wx	Waxy gene (in relation to starch synthesis)
Mins	Minutes
NILs	Near isogenic lines

IGKV	Indira Gandhi KrishiVishwavidyalaya
NaOH	Sodium hydroxide
HCl	Hydrochloric acid
AMG	Amyloglucosidase
GOPOD	Glucose oxidase peroxidase
WUR	Water uptake ratio
KOH	Potassium hydroxide
DEPC	Diethylpyrocarbonate
RT-PCR	Reverse transcription polymerase chain reaction
SNP	Single nucleotide polymorphism
NCBI	National Center for Biotechnology Information
L/W	Length-to-width ratio

References

1. Butardo, V.M., Jr.; Sreenivasulu, N. Improving rice grain quality: State-of-the-art approaches and future prospects. In *Rice Grain Quality: Methods and Protocols*; Springer: Cham, Switzerland, 2016; pp. 139–179. [CrossRef]
2. Tester, R.F.; Karkalas, J.; Qi, X. Starch—Composition, fine structure and architecture. *J. Cereal Sci.* **2004**, *39*, 151–165. [CrossRef]
3. Smith, A.M. The biosynthesis of starch granules. *Biomacromolecules* **2001**, *2*, 335–341. [CrossRef]
4. Asare, E.K.; Jaiswal, S.; Maley, J.; Båga, M.; Sammynaiken, R.; Rossnagel, B.G.; Chibbar, R.N. Barley grain constituents, starch composition, and structure affect starch in vitro enzymatic hydrolysis. *J. Agric. Food Chem.* **2011**, *59*, 4743–4754. [CrossRef]
5. Singh, N.; Singh, J.; Kaur, L.; Sodhi, N.S.; Gill, B.S. Morphological, Thermal and Rheological Properties of Starches from Different Botanical Sources. *Food Chem.* **2003**, *81*, 219–231. [CrossRef]
6. Gao, Z.Y.; Zeng, D.L.; Cui, X.; Zhou, Y.H.; Yan, M.X.; Huang, D.N.; Li, J.Y.; Qian, Q. Map-based cloning of the ALK gene, which controls the gelatinization temperature of rice. *Sci. China Ser. C* **2003**, *46*, 661–668. [CrossRef] [PubMed]
7. Li, H.; Prakash, S.; Nicholson, T.M.; Fitzgerald, M.A.; Gilbert, R.G. The importance of amylose and amylopectin fine structure for textural properties of cooked rice grains. *Food Chem.* **2016**, *196*, 702–711. [CrossRef] [PubMed]
8. Asare, E.K.; Båga, M.; Rossnagel, B.G.; Chibbar, R.N. Polymorphism in the barley granule bound starch synthase 1 (GBSS1) gene associated with grain starch variant amylose concentration. *J. Agric. Food Chem.* **2012**, *60*, 10082–10092. [CrossRef]
9. Nakamura, Y.; Francisco, P.B.; Hosaka, Y.; Sato, A.; Sawada, T.; Kubo, A.; Fujita, N. Essential amino acids of starch synthase IIa differentiate amylopectin structure and starch quality between japonica and indica rice varieties. *Plant Mol. Biol.* **2005**, *58*, 213–227. [CrossRef]
10. Zhang, J.; Zhang, H.; Botella, J.R.; Zhao, Y. Genome editing—Principles and applications for functional genomics research and crop improvement. *Crit. Rev. Plant Sci.* **2017**, *36*, 291–309. [CrossRef]
11. Zhou, H.; Xia, D.; Zhao, D.; Li, Y.; Li, P.; Wu, B.; Gao, G.; Zhang, Q.; Wang, G.; Xiao, J.; et al. The origin of Wx^{la} provides new insights into the improvement of grain quality in rice. *J. Integr. Plant Biol.* **2020**, *63*, 878–888. [CrossRef]
12. Fitzgerald, M.A.; Rahman, S.; Resurreccion, A.P.; Concepcion, J.; Daygon, V.D.; Dipti, S.S.; Kabir, K.A.; Klingner, B.; Morell, M.K.; Bird, A.R. Identification of a Major Genetic Determinant of Glycaemic Index in Rice. *Rice* **2011**, *4*, 66–74. [CrossRef]
13. Kaur, B.; Ranawana, V.; Henry, J. The Glycemic Index of Rice and Rice Products: A Review, and Table of GI Values. *Crit. Rev. Food Sci. Nutr.* **2016**, *56*, 215–236. [CrossRef] [PubMed]
14. Syahariza, Z.A.; Sar, S.; Hasjim, J.; Tizzotti, M.J.; Gilbert, R.G. The importance of amylose and amylopectin fine structures for starch digestibility in cooked rice grains. *Food Chem.* **2013**, *136*, 742–749. [CrossRef]
15. Li, H.; Prakash, S.; Nicholson, T.M.; Fitzgerald, M.A.; Gilbert, R.G. Instrumental measurement of cooked rice texture by dynamic rheological testing and its relation to the fine structure of rice starch. *Carbohydr. Polym.* **2016**, *146*, 253–263. [CrossRef]
16. Anacleto, R.; Cuevas, R.P.; Jimenez, R.; Llorente, C.; Nissila, E.; Henry, R.; Sreenivasulu, N. Prospects of breeding high-quality rice using post-genomic tools. *Theor. Appl. Genet.* **2015**, *128*, 1449–1466. [CrossRef]
17. Juliano, B.O. Rice in human nutrition. Food and Agriculture Organization of the United Nations (FAO). 1993. Available online: https://www.fao.org/4/t0567e/t0567e00.htm (accessed on 2 July 2025).
18. Bao, J. (Ed.) *Rice: Chemistry and Technology*; Elsevier: Amsterdam, The Netherlands, 2018. [CrossRef]
19. Huang, L.; Tan, H.; Zhang, C.; Li, Q.; Liu, Q. Starch biosynthesis in cereal endosperms: An updated review over the last decade. *Plant Commun.* **2021**, *2*, 100237. [CrossRef]
20. Xu, X.; Luo, Q.; Wang, J.; Song, Y.; Ye, H.; Zhang, X.; He, Y.; Sun, M.; Zhang, R.; Shi, G. Large-field objective lens for multi-wavelength microscopy at mesoscale and submicron resolution. *Opto-Electron. Adv.* **2024**, *7*, 230212. [CrossRef]
21. Choe, S.-W.; Kim, B.; Kim, M. Progress of microfluidic continuous separation techniques for micro-/nanoscale bioparticles. *Biosensors* **2021**, *11*, 464. [CrossRef]

22. Qin, F.; Man, J.; Xu, B.; Hu, M.; Gu, M.; Liu, Q.; Wei, C. Structural properties of hydrolyzed high-amylose rice starch by α-amylase from *Bacillus licheniformis*. *J. Agric. Food Chem.* **2011**, *59*, 12667–12673. [CrossRef]
23. Juliano, B.O.; Bautista, G.M.; Lugay, J.C.; Reyes, A.C. Rice quality, Studies on physicochemical properties of rice. *J. Agric. Food Chem.* **1964**, *12*, 131–138. [CrossRef]
24. Megazyme International Ireland Ltd. Total Starch Assay Kit (Amyloglucosidase/Alpha-Amylase Method) Assay Procedure. 2017. Available online: https://www.megazyme.com/total-starch-assay-kit (accessed on 2 July 2025).
25. Goñi, I.; Garcia-Alonso, A.; Saura-Calixto, F. A starch hydrolysis procedure to estimate glycemic index. *Nutr. Res.* **1997**, *17*, 427–437. [CrossRef]
26. Cagampang, G.B.; Perez, C.M.; Juliano, B.O. A gel consistency test for eating quality of rice. *J. Sci. Food Agric.* **1973**, *24*, 1589–1594. [CrossRef]
27. Wu, K.; Gunaratne, A.; Gan, R.; Bao, J.; Corke, H.; Jiang, F. Relationships between cooking properties and physicochemical properties in brown and white rice. *Starch-Starke* **2018**, *70*, 1700167. [CrossRef]
28. Bhattacharya, K.R.; Sowbhagya, C.M. Water uptake by rice during cooking. *Cereal Sci. Today* **1971**, *16*, 420–424. Available online: https://www.cabidigitallibrary.org/doi/full/10.5555/19721607559 (accessed on 2 July 2025).
29. Fraser, B.M.; Verma, S.S.; Muir, W.E. Some physical properties of fababeans. *J. Agric. Eng. Res.* **1978**, *23*, 53–57. [CrossRef]
30. Hirochika, H.; Guiderdoni, E.; An, G.; Hsing, Y.-I.; Eun, M.Y.; Han, C.-D.; Upadhyaya, N.M.; Ramachandran, S.; Zhang, Q.; Pereira, A.; et al. Rice mutant resources for gene discovery. *Plant Mol. Biol.* **2004**, *54*, 325–334. [CrossRef]
31. Zhong, Y.; Blennow, A.; Kofoed-Enevoldsen, O.; Jiang, D.; Hebelstrup, K.H. Protein Targeting to Starch 1 is essential for starchy endosperm development in barley. *J. Exp. Bot.* **2018**, *70*, 485–496. [CrossRef]
32. Yamanouchi, H.; Nakamura, Y. Organ specificity of isoforms of starch branching enzyme (Q-enzyme) in rice. *Plant Cell Physiol.* **1992**, *33*, 985–991. [CrossRef]
33. Kubo, A.; Fujita, N.; Harada, K.; Matsuda, T.; Satoh, H.; Nakamura, Y. The starch-debranching enzymes isoamylase and pullulanase are both involved in amylopectin biosynthesis in rice endosperm. *Plant Physiol.* **1999**, *121*, 399–410. [CrossRef] [PubMed]
34. Utsumi, Y.; Utsumi, C.; Sawada, T.; Fujita, N.; Nakamura, Y. Functional diversity of isoamylase oligomers: The ISA1 homo-oligomer is essential for amylopectin biosynthesis in rice endosperm. *Plant Physiol.* **2011**, *156*, 61–77. [CrossRef] [PubMed]
35. Yu, T.-S.; Zeeman, S.C.; Thorneycroft, D.; Fulton, D.C.; Dunstan, H.; Lue, W.-L.; Hegemann, B.; Tung, S.-Y.; Umemoto, T.; Chapple, A.; et al. Alpha-amylase is not required for breakdown of transitory starch in Arabidopsis leaves. *J. Biol. Chem.* **2005**, *280*, 9773–9779. [CrossRef]
36. Peng, C.; Wang, Y.; Liu, F.; Ren, Y.; Zhou, K.; Lv, J.; Zheng, M.; Zhao, S.; Zhang, L.; Wang, C.; et al. *FLOURY ENDOSPERM6* encodes a CBM48 domain-containing protein involved in compound granule formation and starch synthesis in rice endosperm. *Plant J.* **2014**, *77*, 917–930. [CrossRef]
37. Borule, T.; Pandey, V.K.; Singh, L.; Sathe, A.P.; Akanksha; Raut, P.M.; T.G., A.; Rana, S.S.; Shori, S.; Verulkar, S.B.; et al. Analysis of yield stability in diverse rice genotypes. *J. Adv. Biol. Biotechnol.* **2024**, *27*, 79–89. [CrossRef]
38. Ramadoss, B.R.; Gangola, M.P.; Agasimani, S.; Jaiswal, S.; Venkatesan, T.; Sundaram, G.R.; Chibbar, R.N. Starch granule size and amylopectin chain length influence starch in vitro enzymatic digestibility in selected rice mutants with similar amylose concentration. *J. Food Sci. Technol.* **2019**, *56*, 391–400. [CrossRef] [PubMed]
39. Chung, H.-J.; Liu, Q.; Lee, L.; Wei, D. Relationship between the structure, physicochemical properties and in vitro digestibility of rice starches with different amylose contents. *Food Hydrocoll.* **2011**, *25*, 968–975. [CrossRef]
40. Wang, L.; Yu, X.; Yang, Y.; Chen, X.; Wang, Q.; Zhang, X.; Ran, L.; Xiong, F. Morphology and physicochemical properties of starch in wheat superior and inferior grains. *Starch-Starke* **2018**, *70*, 1700177. [CrossRef]
41. Zhao, F.; Jing, L.; Wang, D.; Bao, F.; Lu, W.; Wang, G. Grain and starch granule morphology in superior and inferior kernels of maize in response to nitrogen. *Sci. Rep.* **2018**, *8*, 6343. [CrossRef]
42. Dhital, S.; Warren, F.J.; Butterworth, P.J.; Ellis, P.R.; Gidley, M.J. Mechanisms of Starch Digestion by α-Amylase—Structural Basis for Kinetic Properties. *Crit. Rev. Food Sci. Nutr.* **2016**, *57*, 875–892. [CrossRef]
43. Chaichoompu, E.; Ruengphayak, S.; Wattanavanitchakorn, S.; Wansuksri, R.; Yonkoksung, U.; Suklaew, P.O.; Chotineeranat, S.; Raungrusmee, S.; Vanavichit, A.; Toojinda, T.; et al. Development of Whole-Grain Rice Lines Exhibiting Low and Intermediate Glycemic Index with Decreased Amylose Content. *Foods* **2024**, *13*, 3627. [CrossRef]
44. Xu, H.; Xu, S.; Xu, Y.; Jiang, Y.; Li, T.; Zhang, X.; Yang, J.; Wang, L. Relationship between the physicochemical properties and amylose content of rice starch in rice varieties with the same genetic background. *J. Cereal Sci.* **2024**, *118*, 103932. [CrossRef]
45. Foster-Powell, K.; Holt, S.C.; Brand-Miller, J.C. International table of glycemic index and glycemic load values: 2002. *Am. J. Clin. Nutr.* **2002**, *76*, 5–56. [CrossRef]
46. Jenkins, D.J.; Wolever, T.M.; Taylor, R.H.; Barker, H.; Fielden, H.; Baldwin, J.M.; Bowling, A.C.; Newman, H.C.; Jenkins, A.L.; Goff, D.V. Glycemic index of foods: A physiological basis for carbohydrate exchange. *Am. J. Clin. Nutr.* **1981**, *34*, 362–366. [CrossRef] [PubMed]

47. Fitzgerald, M.A.; McCouch, S.R.; Hall, R.D. Not Just a Grain of Rice: The Quest for Quality. *Trends Plant Sci.* **2009**, *14*, 133–139. [CrossRef] [PubMed]
48. Cuevas, R.P.; Fitzgerald, M.A. Genetic Diversity of Rice Grain Quality. In *Genetic Diversity in Plants*; InTech: Rijeka, Croatia, 2012. [CrossRef]
49. Singh, S.; Singh, N.; Isono, N.; Noda, T. Relationship of granule size distribution and amylopectin structure with pasting, thermal, and retrogradation properties in wheat starch. *J. Agric. Food Chem.* **2010**, *58*, 1180–1188. [CrossRef] [PubMed]
50. Gong, D.; Zhang, X.; He, F.; Chen, Y.; Li, R.; Yao, J.; Zhang, M.; Zheng, W.; Yu, G. Genetic improvements in rice grain quality: A review of elite genes and their applications in molecular breeding. *Agronomy* **2023**, *13*, 1375. [CrossRef]
51. Zhou, Y.; Miao, J.; Gu, H.; Peng, X.; Leburu, M.; Yuan, F.; Gu, H.; Gao, Y.; Tao, Y.; Zhu, J.; et al. Natural variations in *SLG7* regulate grain shape in rice. *Genetics* **2015**, *201*, 1591–1599. [CrossRef]
52. Custodio, M.C.; Cuevas, R.P.; Ynion, J.; Laborte, A.G.; Velasco, M.L.; Demont, M. Rice quality: How is it defined by consumers, industry, food scientists, and geneticists? *Trends Food Sci. Technol.* **2019**, *92*, 122–137. [CrossRef]